International Journal of Nanomedicine

Dovepress
open access to scientific and medical research

Open Access Full Text Article

ORIGINAL RESEARCH

Treating cancer stem cells and cancer metastasis using glucose-coated gold nanoparticles

This article was published in the following Dove Press journal:
International Journal of Nanomedicine
16 March 2015
Number of times this article has been viewed

Chenxia Hu[1]
Martin Niestroj[2,3]
Daniel Yuan[4]
Steven Chang[5]
Jie Chen[5,6]

[1]Faculty of Chinese Pharmaceutical Science, Guangzhou University of Chinese Medicine, Guangzhou, People's Republic of China; [2]Canadian Light Source, Saskatoon, SK, Canada; [3]Physics Department, Bonn University, Bonn, Germany; [4]Biomedical Engineering Department, Johns Hopkins University, Baltimore, MD, USA; [5]Faculty of Engineering, University of Alberta, Edmonton, AB, Canada; [6]Canadian National Research Council/National Institute for Nanotechnology, Edmonton, AB, Canada

Abstract: Cancer ranks among the leading causes of human mortality. Cancer becomes intractable when it spreads from the primary tumor site to various organs (such as bone, lung, liver, and then brain). Unlike solid tumor cells, cancer stem cells and metastatic cancer cells grow in a non-attached (suspension) form when moving from their source to other locations in the body. Due to the non-attached growth nature, metastasis is often first detected in the circulatory systems, for instance in a lymph node near the primary tumor. Cancer research over the past several decades has primarily focused on treating solid tumors, but targeted therapy to treat cancer stem cells and cancer metastasis has yet to be developed. Because cancers undergo faster metabolism and consume more glucose than normal cells, glucose was chosen in this study as a reagent to target cancer cells. In particular, by covalently binding gold nanoparticles (GNPs) with thio-PEG (polyethylene glycol) and thio-glucose, the resulting functionalized GNPs (Glu-GNPs) were created for targeted treatment of cancer metastasis and cancer stem cells. Suspension cancer cell THP-1 (human monocytic cell line derived from acute monocytic leukemia patients) was selected because it has properties similar to cancer stem cells and has been used as a metastatic cancer cell model for in vitro studies. To take advantage of cancer cells' elevated glucose consumption over normal cells, different starvation periods were screened in order to achieve optimal treatment effects. Cancer cells were then fed using Glu-GNPs followed by X-ray irradiation treatment. For comparison, solid tumor MCF-7 cells (breast cancer cell line) were studied as well. Our irradiation experimental results show that Glu-GNPs are better irradiation sensitizers to treat THP-1 cells than MCF-7 cells, or Glu-GNPs enhance the cancer killing of THP-1 cells 20% more than X-ray irradiation alone and GNP treatment alone. This finding can help oncologists to design therapeutic strategies to target cancer stem cells and cancer metastasis.

Keywords: glucose capped gold nanoparticles, cancer metastasis, cancer stem cells, irradiation therapy, targeted treatment, suspension cancer cells

Introduction

Cancer can originate in various organs as its primary location in the body. Cancer metastasis occurs when cancer cells spread from their original location to a new location or different organs. For instance, lung cancer can migrate from its primary site (eg, the lungs) to a new location (eg, the bones). One of the possible mechanisms of cancer metastasis is that cancer cells break off from its original tumor and enter the blood and the lymphatic systems. These metastatic cancer cells can sometimes insidiously evade detection by the immune system and are carried by the blood stream or lymphatic fluid to a new location in the body.[1] Stephen Paget in 1889 proposed that metastasis happens because interactions between "seed" (or cancer cells) and "soil" (or the specific organ microenvironments or metastatic niche).[2,3]

Correspondence: Jie Chen
Faculty of Engineering, University of Alberta, ECERF W6-019, 9107-116 Street, Edmonton, AB T6G 2V4, Canada
Tel +1 780 492 9820
Email jc65@ualberta.ca

Cells that can migrate may not metastasize because they might lack the ability to invade through the extracellular matrix.[4] Therefore, migration and metastasis are completely different. Circulation is not the only reason behind metastasis. Cancer cells survive and grow by angiogenesis, the process of building a new blood supply. Cancer can spread almost anywhere in the body, but the most common sites of metastasis are the bones, the brain, the liver, and the lungs because these tissues are well vascularized with blood veins that metastatic cells can be carried through. Patients may experience no or few symptoms even when cancer starts to migrate, but it becomes very difficult to treat once cancer spreads.[5] In some cases, the metastatic tumor is found during routine examinations or tests before the primary tumor is detected. Therefore, treating cancer metastasis becomes extremely important.

Cancer stem cells, like normal stem cells, have the ability to renew themselves and give rise to all cancer cell types. They share key behavioral characteristics of suspension growth cells[6] as they proliferate through the bloodstream during cancer recidivism and metastasis, ultimately giving rise to new tumors. Designing a specific targeted therapy to treat cancer stem cells becomes critical to improve the survival and quality of life of cancer patients, especially those already experiencing cancer metastasis.

Current clinical cancer treatments (either radiation therapy or chemotherapy) are "blind" in that harmful chemicals or ionizing radiation affects the whole treated area regardless of whether the tissue in the area is benign or malignant. Nanotechnology, which has been advanced significantly over the past several decades,[7,8] offers a new targeted-cancer-treatment which attacks cancerous cells with reduced harmful side effects suffered by surrounding normal cells. Nanoparticles are usually made of inorganic nanomaterials such as gold nanoparticles (GNPs). These nanoparticles themselves often lack pathology targeting mechanisms, and thus various functional biomolecules (eg, cancer targeted ligands) are required to bind with nanoparticles to make them functional nanoparticles. Many studies have shown that functional nanoparticles are more effective in treating cancers and improving cellular targeting and X-ray irradiation sensitization than nanoparticles alone.[7,9–11] Among these nanoparticles, biocompatible GNPs are the only US Food and Drug Administration (FDA) approved nanomaterials for clinical trials.[12] Many researchers have also shown that GNPs are promising candidates for various biomedical applications in cancer diagnostics and therapeutics.[13–15] For instance, GNPs in combination with surface plasmon resonance and surface enhanced Raman scattering increase the sensitivity of imaging systems.[16–19] GNPs were also used for other therapeutic applications, such as targeted drug delivery.[20–25] One cancer killing mechanism study indicates that GNPs effectively increase the absorption of radiation leading to thermal denaturation and coagulation of cancerous cells as a result of surface plasmon resonance.[26] The other more commonly accepted cancer-killing mechanism is that GNPs enhance sensitization of irradiation at megavoltage energies due to increased free radicals of gold, the photoelectric effect, and the Compton effect.[27–31] Consequently, the more GNPs taken up by cancer cells, the better the therapeutic outcome during irradiation. Although GNPs have shown improvement over irradiation treatment alone, their targeting ability relies on differential amounts of GNPs taken up by cancerous cells compared to surrounding normal cells. Therefore, we need to choose biomolecules that modify the surface of GNPs so that they are more attractive to cancer cells.

Cancer cells reproduce more rapidly and live longer than normal cells because they utilize specific proteins and glucose to support their continuous growth.[32] One of the most attractive properties of GNPs is their ability to covalently conjugate with various biomolecules via thiol groups.[14] GNPs capped with suitable functional biomolecules can enhance their uptake by cancer cells but not surrounding normal cells eg, macrophages, endothelial cells,[33,34] thereby becoming attractive for tumor detection and therapy.[9,35–38] Glucose is a primary source of metabolic energy for cells, thus cancer cells take significantly more glucose compared to normal cells. Specifically, larger numbers of glucose molecules are internalized via GLUT receptors present on cancer cell surfaces.[39,40] Glucose tagging is, therefore, an effective way to facilitate the entry of GNPs into cells. In vitro and in vivo studies show that pegylated glucose coated GNPs (or Glu-GNPs) of 20 nm in diameter are more effective in targeting solid cancer (ie, breast, liver, prostate, and ovarian cancers).[9,10,30] In addition, images showed that Glu-GNPs enter cancer cells more than surrounding normal cells in our animal studies.[41,42] Although the therapeutic effectiveness of Glu-GNPs versus (vs) naked GNPs has attracted wide research interest, the majority of research has focused on the uptake of nanoparticles in solid tumors or attached-growing cells, such as MCF-7 and HeLa cells. To the best of our knowledge, no report has been published on evaluating cellular uptake of Glu-GNPs vs naked GNPs for suspension cells (lymphoma cells, leukemia cells, metastatic cancer cells or even cancer stem cells).

Materials and methods

Chemicals and materials

Gold (III) chloride trihydrate ($HAuCl_4 \cdot 3H_2O$), trisodium citrate sodium ($Na_3C_6H_5O_7 \cdot 2H_2O$), 1-thio-D-glucose (Glu) and thio-polyethylene glycol (thio-PEG with the molecular weight of 5,000 g/mol) were purchased from Sigma-Aldrich Co., St Louis, MO, USA. All the materials were dissolved in deionized water purified by the Milli-*Q* Biocel system (ZMQS50F01; Millipore, USA).

Synthesis of Glu-GNPs and GNPs

There were two main steps involved in GNP and Glu-GNP synthesis:

- Making stock solutions: 3 mL of 25 mM Gold (III) chloride trihydrate ($HAuCl_4 \cdot 3H_2O$) was added to 47 mL of deionized water in a clean Erlenmeyer flask. Using a magnetic stir bar, the solution was stirred at 350 rpm on a magnetic hot plate at 300°C. A reflux column was used as a condenser to prevent the evaporated water from escaping. Eight milliliters of 34 mM trisodium citrate was rapidly added to the solution as a reducing agent once condensation was seen in the reflux column. The solution was heated for another 2 minutes until the color of the solution turned dark red. After heating, the solution was stirred for another 20 minutes to allow the reaction to complete.
- Making the final solutions: i) because GNPs in the previously made stock solutions can aggregate, they were stabilized by coating with thio-PEG. To make stabilized GNPs for in vitro experiments, thio-PEG was added to the previously prepared stock solution and mixed. ii) To make Glu-GNPs, both thio-PEG and thio-glucose were added to previously prepared stock solutions of GNPs and mixed well. Note that both glucose and PEG are covalently bound onto GNPs, and the molar ratio is PEG:Au:glucose =0.06:1:0.687.

The samples were finally purified by centrifugation for 30 minutes and the supernatant was discarded.

Characterization of nanoparticles and cellular uptake

The following tools were used to characterize nanoparticles and image cellular uptake:

- Transmission electron microscopy (TEM; JEM-100CX) is a technique to image nanoparticles at much higher resolution than that obtained by conventional microscopes. The image is formed due to the interaction of electrons when they pass through the nanoparticles. Ten microliters of GNPs was deposited onto a treated grid. The grid was covered with a petri dish lid and left to stand at room temperature for the chosen capture time, around 15 minutes. Subsequently, the grid was carefully dip-rinsed with deionized water. TEM was used to measure the projected images of GNPs, and thus surface morphology of GNPs could be obtained.
- When light impinges on nanoparticles (GNPs or Glu-GNPs), its photons are scattered in a mathematically predictable manner. Dynamic light scattering (DLS; Zetasizer Nano S, Malvern Instruments, Malvern, UK) is a technique used to determine the size distribution of GNPs or Glu-GNPs in solution. Starting with a GNP solution of 1 mg/mL Au, the concentration was adjusted to accommodate the scattering properties of GNPs and the optical requirement of the instrument. The GNP solution was added into a clean quartz cuvette to ensure liquid level at least 2 mm above the height of the laser beam. The DLS analysis software was used to measure the size distribution of GNPs.
- Atomic force microscopy (AFM; Veeco Multimode V SPM) consists of a cantilever with a sharp tip (probe) made of silicon or silicon nitride. It is often used to scan the specimen surface. GNPs of 25 µL were evenly dispersed on a flat high-quality mica surface. Height calibration was performed before AFM measurements. Because GNPs are bound to the substrate via weak physical forces, intermittent contact mode was chosen for imaging and measurement.
- Scanning electron microscopy (SEM; Carl Zeiss Meditec AG, Jena, Germany) is commonly used to image the morphology of samples using a focused beam of electrons. To capture the morphology of THP-1 cells after treatment with Glu-GNPs and X-ray, the cells were collected and attached to the plates by using poly-L-lysine. The cells were then fixed in 2% glutaraldehyde in a 4% PEA/cacodylate buffer for 2 hours at room temperature. A graded ethanol series (50, 70, 90, and 100%) and a graded mixture series of ethanol and hexamethyldisilazane (75:25, 50:50, and 25:75) were used to dehydrate all the samples. After the dehydration process, the cells were kept overnight in 100% hexamethyldisilazane at room temperature. Thereafter, a Hummer 6.2 sputtering system was used to coat them with gold-palladium. The SEM images were taken by an XL 30 scanning electron microscope (Philips) operated at 20 kV.

Cell culture

Leukemic stem cell, THP-1, was selected in our study because it shares many properties of cancer stem cells.[43]

The clonogenicity of THP-1 cells has been reported,[44] and cell surface markers like CD44 expressed in THP-1 have also been studied.[45] THP-1 is one of the common cell types used for modeling cancer stem cells. In our previous study, we have validated that PEG-Glu-GNPs can enhance the irradiation treatment of solid tumor cells, such as breast cancers,[9] prostate cancers,[30] and ovarian cancer.[11] To compare the therapeutic efficacy of Glu-GNPs with different types of cells, THP-1 and MCF-7 cells were chosen. Note that the breast cancer cell line MCF-7 was selected because it is a commonly used cancer cell line in cancer studies. Both the THP-1 (suspension growth) and MCF-7 (attached growth) cell lines purchased from the American Type Culture Collection (Manassas, VA, USA) were used for the in vitro experiments. Both were cultured in Dulbecco's Modified Eagle's Medium (DMEM) supplemented with 10% fetal bovine serum (Thermo Fisher Scientific, Waltham, MA, USA), 20 mmol/L D-glucose, 100 UI/mL penicillin G, and 100 µg/mL streptomycin (Sigma-Aldrich Co.) in a humidified incubator with 5% CO_2, at 37°C. These cells were then used for the starvation and irradiation tests (refer to Section "Radiation effect on killing cancer cells after nanoparticles uptake").

GNP treatments

Effect of same starvation times on pharmacokinetics of nanoparticle uptake

MCF-7 and THP-1 cells were seeded at approximately ($2.0*10^5$) per well in 35 mm dishes for 18 hours. The medium was then switched to DMEM without glucose (Thermo Fisher Scientific) for 2 hours. Glu-GNPs and naked GNPs (10 µL per 1 mL medium) were added into the medium afterward. The same amount of DI water was added as the control. The cells were collected at different time points, 1 hour, 2 hours, 3 hours, and 4 hours afterward (Figure 1). The reason tests did not go beyond 4 hours is that cells reached the peak concentration of Glu-GNP uptake and started to expel Glu-GNPs thereafter (refer to the Results and Discussion sections and Figure 2).

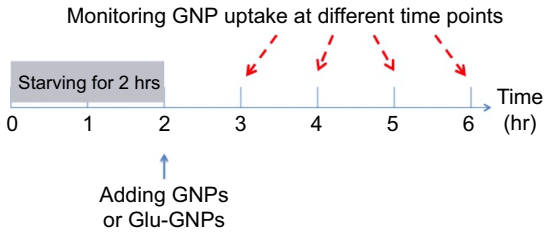

Figure 1 Experimental design to check cells' uptake of nanoparticles with 2-hour starvation.
Abbreviations: GNPs, gold nanoparticles; Glu-GNPs, pegylated glucose coated GNPs.

Medium was then removed and the cells were washed with phosphate-buffered saline twice. After washing, the cells were digested with 0.3 mL of trypsin and suspended in 1 mL of DMEM without glucose. The cells were counted using a hemocytometer. After counting, the cells were centrifuged and supernatant was removed. A half milliliter of HCl:HNO_3 (3:1) (concentrated 34% HCl mixed with 68% HNO_3) was added to each sample to lyse the cells. The final gold mass in each solution was measured using inductively coupled plasma mass spectrometry (ICP-MS or ICP-AES). Knowing the concentration of gold and the number of cells in the solution, cellular uptake of GNPs could be calculated by dividing the concentration of GNPs by the number of cells in the solution based on the hemocytometer counting results.

Effect of different starvation times on pharmacokinetics of nanoparticle uptake

In previous tests, the starvation time was set constant at 2 hours to check whether deprivation of glucose can help Glu-GNP or even GNP uptake. The following tests were designed to screen the optimal starvation time (or what is the best starvation time so that cells take up the maximum amount of Glu-GNPs. The design is quite similar to the previous one. MCF-7 and THP-1 cells were seeded at approximately ($2.0*10^5$) per well in 35 mm dishes each for 18 hours. The medium was switched to DMEM without glucose. After different starvation times (1 hour, 2 hours, and 3 hours), Glu-GNPs and naked GNPs (10 µL per 1 mL medium) were added to the medium. The hypothesis is that cancer cells consume more glucose capped GNPs and starvation can help nanoparticle uptake. However, the starvation could not go beyond 3 hours otherwise cells became unhealthy. Based on the previous studies,[9,11,30] 1 hour or 2 hours after incubation was the optimal cellular uptake time of GNPs and Glu-GNPs. Cells started to expel GNPs if the incubation time was longer. The cells were collected at 1 hour and 2 hours after incubation with Glu-GNPs and naked GNPs (refer to Figure 3). The process of cell uptake assay for the MCF-7 and THP-1 cells was the same as mentioned previously.

Irradiation

MCF-7 and THP-1 cells were seeded at approximately $2*10^5$ per well in 35 mm culture dishes for 18 hours. The medium was then switched to DMEM without glucose for 2 hours. Depending on the study group, either Glu-GNPs or naked GNPs (10 µL per 1 mL medium) were subsequently added into the medium. The same volume of DI water was added

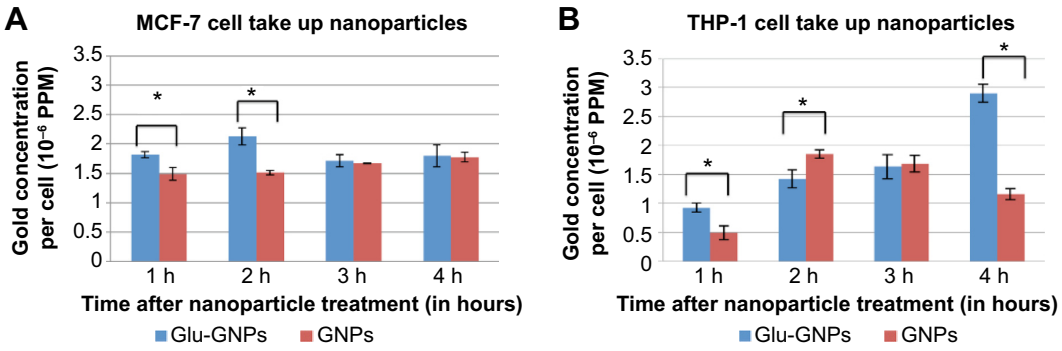

Figure 2 Uptake of nanoparticles.
Notes: (**A**) Nanoparticles taken up by MCF-7 cells: average and standard deviations; (**B**) Nanoparticles taken up by THP-1 cells: average and standard deviations. Note that 1 h on the horizontal axis designates 1 hour after cells were treated by nanoparticles. *Indicates a significant difference ($P<0.05$) when comparing gold concentration of cells treated with Glu-GNPs or GNPs.
Abbreviations: GNPs, gold nanoparticles; Glu-GNPs, pegylated glucose coated GNPs.

to the control group. One hour later, the medium containing GNPs was removed. The cells were washed twice with phosphate-buffered saline and then replenished with fresh medium with glucose. Both GNP treated and untreated cells were then irradiated with 200 kVp X-rays of 0, 6, and 9 Gy. Note that Gy is the SI unit for absorbed dose with the units of joules/kilogram (1 joule $=6.24*10^{18}$ eV). After irradiation, the cells were collected for a cell proliferation assay (MTS). MCF-7 and THP-1 cells were separately seeded with $2.0*10^{3}$ cells per well in a 96-well culture plate. The experiments were repeated in triplicate. The cells without nanoparticles and the cells without irradiation served as the controls. When the cells were incubated at 36, 60, and 84 hours after X-ray treatment, cell viability was measured using the MTS assay and the results were also confirmed using the traditional cell count method. The results for cellular survival in response to Glu-GNPs and GNPs with and without irradiation were determined using the ELx800 Absorbance Microplate Reader (BioTek, USA) and the absorbance values at 490 nm were recorded at the indicated time points.

Statistical analysis

Experimental values were determined in triplicate. All values regarding measurement and percentage of gold content were expressed as mean and standard deviation. The one-way analysis of variance (ANOVA) and Tukey's multiple comparison post-tests were used. Differences less than 0.05 ($P<0.05$) were considered statistically significant.

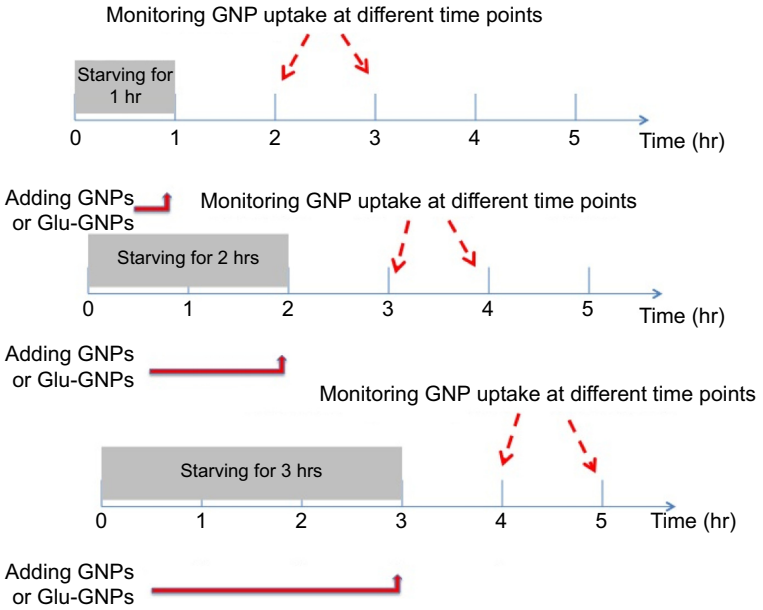

Figure 3 Experimental design to check cells' uptake of nanoparticles with different starvation times.
Abbreviations: GNPs, gold nanoparticles; Glu-GNPs, pegylated glucose coated GNPs; hr, hour(s).

Results and discussion

Characterization of GNPs

The morphology of Glu-GNPs was imaged using TEM (refer to Figure 4A). The diameters of the Glu-GNPs and their size distribution were measured using DLS and AFM (refer to Figure 4B). The average diameter of these nanoparticles was around 20 nm (Glu-GNPs and GNPs are of a similar size around 20 nm because glucose is a small molecule and thus does not make a noticeable size difference). Most studies show that GNPs of small size (<50 nm) can easily enter cells without causing much damage.[12] We chose a nanoparticle size of 20 nm because our previous in vivo and in vitro studies showed that Glu-GNPs of 20 nm are more effective in treating cancer and being discharged from the body afterward.[42,46]

Cellular uptake of Glu-GNPs and GNPs in targeted cells

In vivo experiments have shown that Glu-GNPs can be taken up by solid tumors under normal glucose conditions (without starvation).[42,46] In this in vitro study, we seek to examine how starvation impacts the cellular uptake of Glu-GNPs by cancer stem cells. Our premise is that patients being starved prior to Glu-GNP plus X-ray treatment can achieve a better targeted tumor-killing effect than those without starvation. The experiments were carried out in two groups: i) cellular uptake tests with the same starvation time (2 hours); and ii) cellular uptake tests with different starvation times.

Cellular uptake of nanoparticles after 2-hour starvation

Taking cells prepared according to the procedure outlined in "Characterization of nanoparticles and cellular uptake", both MCF-7 cells and THP-1 cells were cultured in DMEM without glucose (Thermo Fisher Scientific), and were deprived from glucose or were starved for 2 hours. They were then treated with Glu-GNPs and GNPs. Nanoparticle metabolism was monitored at different time points (1 hour, 2 hours, 3 hours, and 4 hours) after treatments (refer to Figure 1). GNPs were able to enter the cytoplasm of both types of cells (Figure 4C) and a few even entered the nuclei of cells. Gold concentration per cell was calculated based on the total gold concentration measured by ICP-AES divided by the total living cell number counted by the hemocytometer, shown in Figure 2A and B.

For MCF-7 cells, we notice from Figure 2A: i) the uptake of GNPs gradually increased as time elapsed from 1 hour to 4 hours. The hypothesis is that, a gold concentration gradient causes GNPs to gradually diffuse into the cells. ii) The uptake of Glu-GNPs, on the other hand, increased quickly and peaked at 2 hours. The hypothesis is that glucose is the main energy source for cell growth. After 2 hours of starvation, cells urgently needed glucose to maintain their metabolism. They took up Glu-GNPs during the first 2 hours resembling the uptake of pure glucose. However, Glu-GNPs exhibited different pharmacokinetics compared to glucose. Cells started to expel Glu-GNPs, evident in their decreased concentration after 2 hours. Three hours after nanoparticle

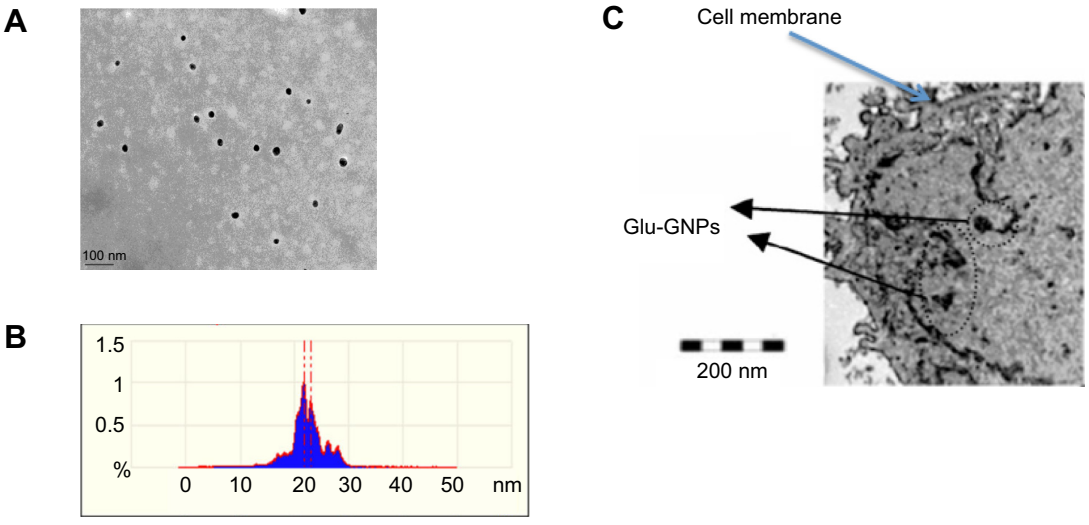

Figure 4 Characteristics of Glu-GNPs.
Notes: (**A**) TEM picture of Glu-GNPs and (**B**) the size distribution of Glu-GNPs measured by atomic force microscopy. The y-axis shows the percentage of nanoparticles falling into a particular size range and the x-axis shows the measured size of nanoparticles. For example, as indicated by the first red dashed line, nanoparticles with diameters around 22 nm account for 1% of all the particles measured. (**C**) TEM picture show Glu-GNPs entering cancer cells and in cytoplasm.
Abbreviations: GNPs, gold nanoparticles; Glu-GNPs, pegylated glucose coated GNPs; TEM, transmission electron microscopy.

treatment, gold concentration in cells matched that of GNPs alone. Note that long chain PEGs (molecular weight, MW =5,000) could mask small molecules (like glucose) conjugated to the GNPs' surface rendering them less effective. In other words, once glucose molecules were covered by PEGs, the targeting efficiency gained by using glucose as a cancer targeting agent got lost. To alleviate the problem, the molar ratio PEG:Au:glucose =0.06:1:0.687 was adjusted accordingly – ten times more glucose than PEG.

Cellular uptake behavior varies depending on cell types and their growth conditions (attached vs suspension growth). For THP-1 cells, the effect of glucose functionalization on cellular uptake is more dramatic than that of MCF-7 cells, reflected in Figure 2B. The uptake of GNPs on THP-1 decreased 2 hours after the nanoparticle treatment (from $1.8*10^{-6}$ PPM at 2 hours to $1.6*10^{-6}$ PPM at 3 hours then to $1.1*10^{-6}$ PPM at 4 hours shown in Figure 2B). THP-1 cells endocytosed GNPs during the first 2 hours, but cells realized GNPs were unwanted substances and expelled GNPs after 2 hours. The amount of Glu-GNPs in THP-1 cells was comparable to that of Glu-GNPs in MCF-7 cells, $1.6*10^{-6}$ PPM at 3 hours. Although the amount of Glu-GNPs was lower at 1 and 2 hours after nanoparticle treatment ($0.95*10^{-6}$ PPM at 1 hour and $1.48*10^{-6}$ PPM at 2 hours), but it caught up 3 and 4 hours after nanoparticle treatment ($1.6*10^{-6}$ PPM at 3 hours and $2.9*10^{-6}$ PPM at 4 hours refer to Figure 2B). The uptake of Glu-GNPs vs that of GNPs in THP-1 cells at 4 hours was drastically different ($2.90*10^{-6}$ PPM vs $1.15*10^{-6}$ PPM) mainly due to the glucose coating. THP-1 cells cannot distinguish Glu-GNPs from glucose and continue to take up Glu-GNPs. This is exactly what we wanted to achieve: Glu-GNPs exhibit superior differential uptake by cancer cells compared to surrounding normal cells (computed tomography and positron emission tomography images in our previous in vivo studies[42,46] confirmed this finding). Considering that THP-1 cells are smaller to MCF-7 cells, the density of Glu-GNPs in THP-1 cells was actually higher than that in MCF-7 cells. Here density is defined as the mass of GNPs in each cell divided by cell volume (the average diameter of MCF-7 cells is about 18±2 μm,[47] while the average diameter of THP-1 cells is about 7±2 μm based on our measurement [refer to Figure 5D]). This phenomenon can be explained

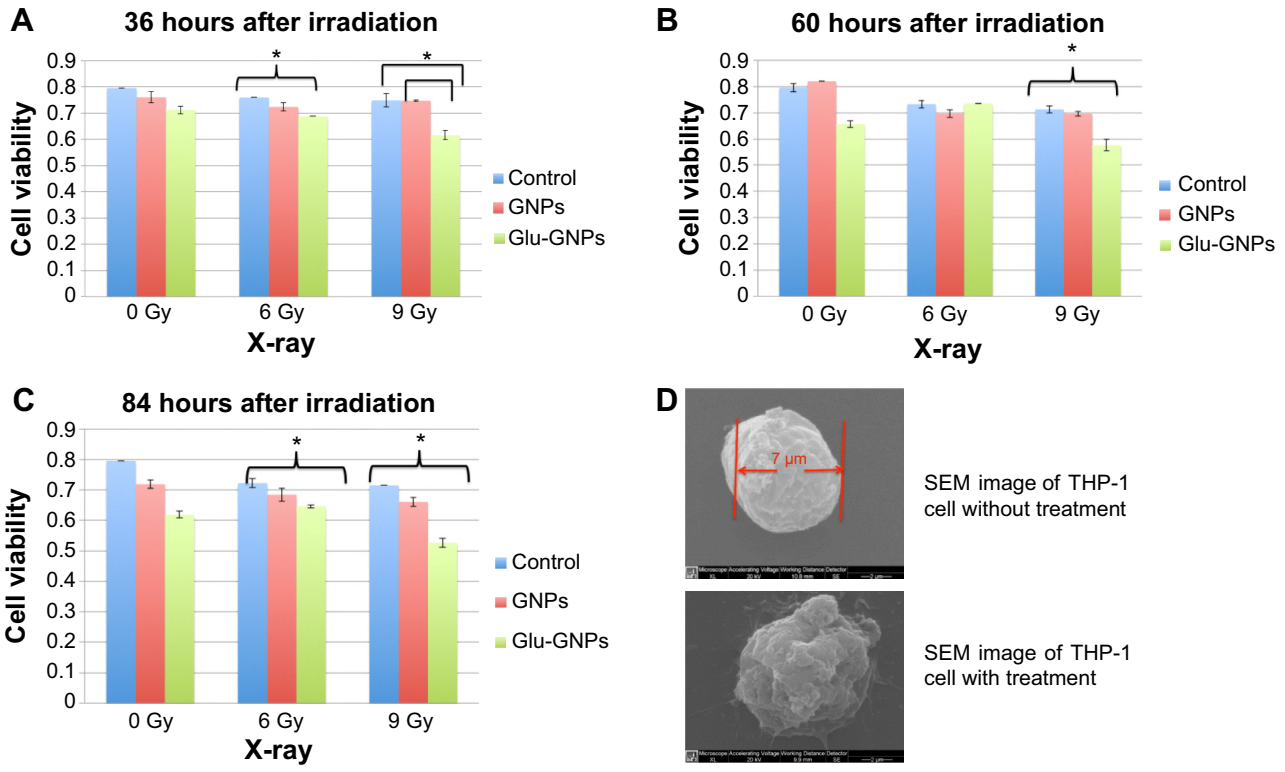

Figure 5 THP-1 cell viability.

Notes: THP-1 cell viability measured by MTS assay at 36 hours (**A**), 60 hours (**B**), and 84 hours (**C**) after irradiation. *Indicates that a significant difference ($P<0.05$) was shown when comparing gold concentration in cells treated with Glu-GNPs versus GNPs. Note that 0.9 on the y-axis stands for a cell viability of 90%. (**D**) Scanning electron microscopy (SEM) images of THP-1 cells: with and without treatment. The average diameter of THP-1 cells is about 7±2 μm.

Abbreviations: GNPs, gold nanoparticles; Glu-GNPs, pegylated glucose coated GNPs.

as follows: THP-1 cells, unlike MCF-7 cells, are suspension growth cells. The proportional surface area of these cells, which is in contact with the Glu-GNP medium, is much larger than that of attached growth MCF-7 cells (the attached side, in theory, is only in contact with the adjacent cells or tissues). Therefore, results show higher Glu-GNP density in THP-1 cells. After starving for 2 hours, cellular uptake of Glu-GNPs by THP-1 cells continued to increase and reached a peak level of $2.9*10^{-6}$ PPM at 4 hours. This behavior is totally different from that of MCF-7 cells for which uptake peaked at 2 hours after Glu-GNP treatment at about $2.1*10^{-6}$ PPM. From this study, THP-1 cells more favorably take up Glu-GNPs than MCF-7 cells.

Cellular uptake of nanoparticles with different starvation durations

Starvation helps with GNP uptake, especially for suspension cells. This can be clearly observed from the previous studies. However, the optimal starvation duration has yet to be determined. The following experiments were designed to investigate uptake dynamics over time. MCF-7 cells and THP-1 cells were cultured separately in the DMEM without glucose for 1 hour, 2 hours, and 3 hours. Cells were separately treated with Glu-GNPs and naked GNPs afterward. The cells were then collected 1 hour and 2 hours after incubation so that the concentration of GNPs in the cells could be measured (refer to the drawing in Figure 3).

For the MCF-7 cells, the nanoparticle uptake results with different starvation durations are shown in Figure 6. The following observations were made: i) MCF-7 cells starved for 1 hour kept taking up Glu-GNPs and GNPs (refer to Figure 6A). The observation indicates that cancer cells experienced fast metabolism and were inclined to consume more glucose. This observation is also in line with the other reported findings.[48] ii) Although MCF-7 cells starved for 2 hours kept taking up Glu-GNPs (refer to Figure 6B), the uptake rate (in units of gold concentration increase per hour) was not as great as that of the cells starved for 1 hour. For naked GNPs, cells did not take up any more GNPs as the amount of GNPs reached an equilibrium state (refer to Figure 6B). iii) For MCF-7 cells starved for 3 hours, Glu-GNPs in cells decreased instead of increased (from $2.0*10^{-6}$ PPM to $1.0*10^{-6}$ PPM, refer to Figure 6C). The concentrations of GNPs also declined slightly (around $1.5*10^{-6}$ PPM). From the previous studies (refer to the results in Figure 6), the optimal starvation duration for MCF-7 cells is between 1 and 2 hours.

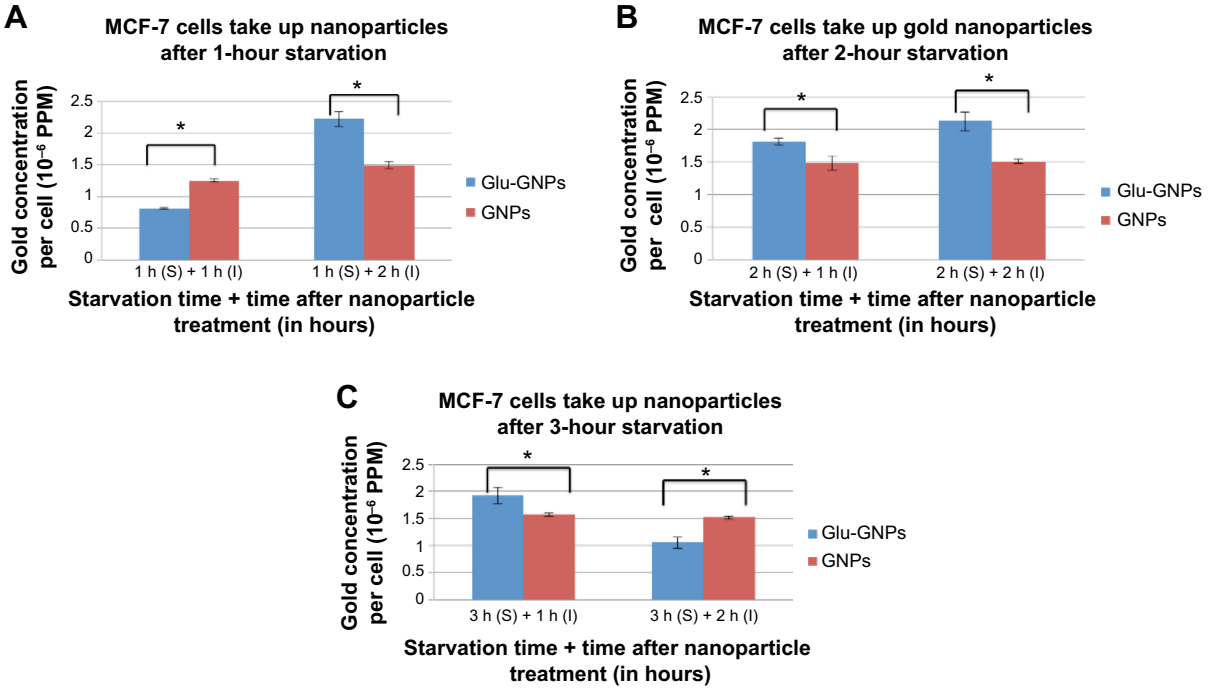

Figure 6 GNPs taken up by MCF-7 cells after different starvation durations.
Notes: (**A**) The average GNP uptake amount by MCF-7 cells after 1 hour of starvation. (**B**) After 2 hours of starvation, and (**C**) after 3 hours of starvation. Note that on the horizontal axes of these figures, the notation "S" stands for "starvation" and "I" stands for "incubation after nanoparticle treatment". For instance, notation "1 h (S) + 1 h (I)" denotes that cells were starved for 1 hour, treated by nanoparticles and then incubated for 1 hour. *Indicates that a significant difference ($P<0.05$) was shown when comparing gold concentration of cells treated with Glu-GNPs or GNPs.
Abbreviations: GNPs, gold nanoparticles; Glu-GNPs, pegylated glucose coated GNPs.

For THP-1 cells, the nanoparticle uptake results with different starvation durations are shown in Figure 7. The following observations were made: i) for THP-1 cells starved for 1 hour, cells kept taking up Glu-GNPs and GNPs (refer to Figure 7A). More Glu-GNPs than naked GNPs were taken up by the THP-1 cells with longer incubation time. This observation indicates that cancer cells are hungry for glucose, and THP-1 cells behave the same as MCF-7 cells. ii) For THP-1 cells starved for 2 hours, cells kept taking up Glu-GNPs and GNPs. However, the uptake trend differs from that of MCF-7 cells after 2 hours of starvation (in which, uptake of either Glu-GNPs or GNPs more or less reached an equilibrium state). THP-1 cells, on the other hand, have much more potential to take up nanoparticles due to their larger contact area with glucose medium. Cellular uptake of Glu-GNPs by THP-1 cells kept increasing and reached a peak value of $3*10^{-6}$ PPM at 4 hours (2 hour starvation plus 2 hours incubation with glucose medium afterward) according to Figures 2B or 7B. iii) For THP-1 cells starved for 3 hours, cellular uptake of both Glu-GNPs and naked GNPs decreased (refer to Figure 7C), which was the same observation as for MCF-7 cells. The result suggests that cells should not be starved for more than 3 hours. Otherwise, neither Glu-GNPs nor GNPs have any targeted effect on cancer treatment.

Clinical relevance

Suspension THP-1 cancer cells have been used to model cancer stem cells and cancer metastasis.[49] In this study, cellular uptake of Glu-GNPs vs naked GNPs was evaluated using THP-1 as a cancer model. The goal is to investigate whether there is any significant difference in targeted treatment due to the glucose conjugation. In positron emission tomography scans, glucose-capped imaging contrast (Fludeoxyglucose [^{18}F]) is used for imaging. To achieve better imaging results, patients are required to fast for at least 8 hours before a test. Along the same line of thinking, starvation was used in this study as well for achieving better treatment effects. Different durations of starvation were compared to find the optimal dosage response (or maximum Glu-GNP taken up by cancer cells).

From previous experiments, starvation was shown to impact nanoparticle uptake: i) 1- to 2-hour starvation enables both MCF-7 and THP-1 cells to take up more Glu-GNPs, but longer starvation time diminishes the effect. ii) Glu-GNPs, in general, have a stronger effect on THP-1 cells than on

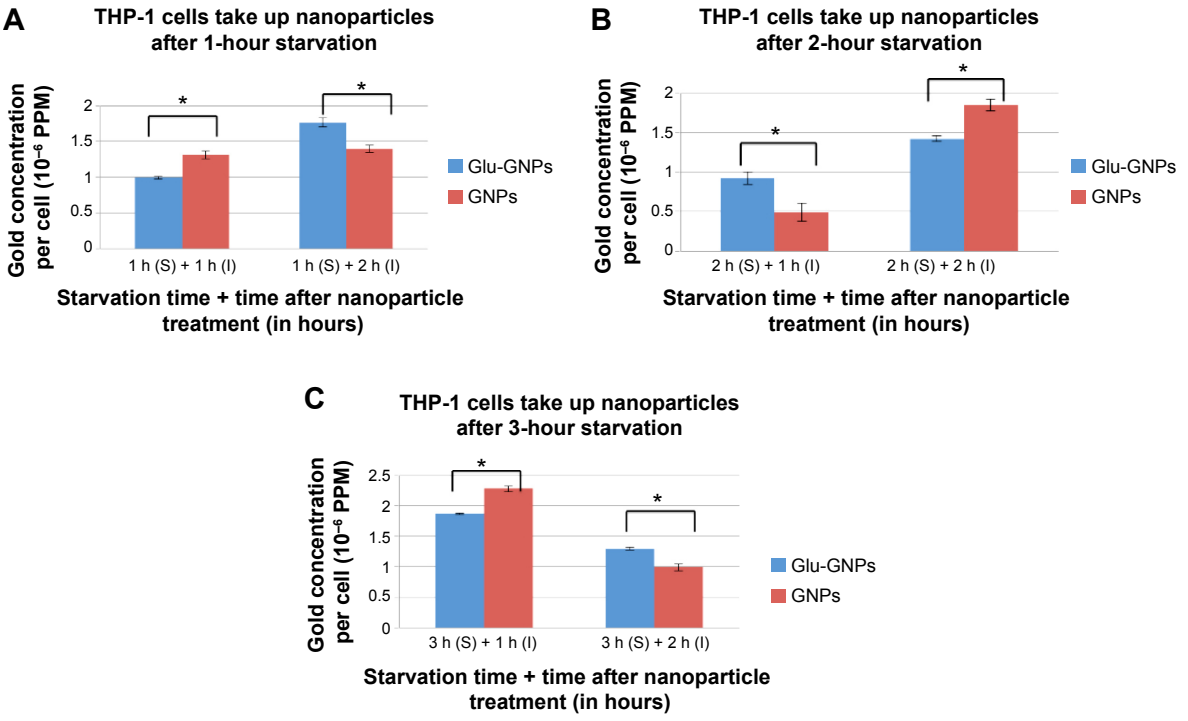

Figure 7 Nanoparticle uptake by THP-1 cells with different starvation durations.

Notes: (**A**) Averaged uptake by THP-1 cells with 1 hour of starvation; (**B**) 2 hours of starvation; and (**C**) 3 hours of starvation. Note that on the horizontal axes of these figures, the notation "S" stands for "starvation" and "I" stands for "incubation after nanoparticle treatment". For instance, notation "1 h (S) + 1 h (I)" denotes that cells were starved for 1 hour, treated by nanoparticles and then incubated for 1 hour. *Indicates that a significant difference ($P<0.05$) was shown when comparing gold concentration of cells treated with Glu-GNPs or GNPs.

Abbreviations: GNPs, gold nanoparticles; Glu-GNPs, pegylated glucose coated GNPs.

MCF-7 cells. This finding is supported by the prevailing theory that cancer cells need more glucose to grow than normal cells documented in textbooks[50,51] and a research article.[47] The layer of glucose on GNPs has successfully achieved the goal of targeted cancer treatment. To our best knowledge, no research group has studied the impact of starvation on Glu-GNPs taken up by suspension cancer cells.

Radiation effect on killing cancer cells after nanoparticles uptake

As mentioned in the introduction, studies have shown GNPs enhance sensitization of irradiation at megavoltage energies.[27] Although the exact mechanisms are unclear, radiosensitization is generally attributed to the fact that GNPs (high Z elements) absorbed radiation and generated free radicals. The resulting transfer of free radicals can selectively enhance radiation therapy efficacy leading to differentially increased tumor cell killing. In what follows, we compare the therapeutic effects of Glu-GNPs on MCF-7 and THP-1 cells, respectively.

Glu-GNPs' enhancement of MCF-7 cell killing

Based on the previous starvation tests (refer to Figures 6 and 7), 1-hour starvation achieved the best Glu-GNP uptake for both MCF-7 and THP-1 cells. As a result, starvation for 1 hour was chosen before the X-ray irradiation tests. Specifically, cells were treated with either Glu-GNPs or naked GNPs after starvation for 1 hour. According to our previous studies,[9,11] cells need at least 24 hours to recover after irradiation. MTS assay at 36, 60, and 84 hours after the irradiation was chosen to check cell viability. The detailed irradiation procedure is listed in "Irradiation" section. For MCF-7 cells, Figure 8A–8C show the cell viability with X-ray irradiation of different intensities at 36, 60, and 84 hours, respectively. The observations are:

- 84 hours after MCF-7 cells were irradiated, the cell viability for the control is 59%, for GNP only is 56%, and for Glu-GNPs is 50% (refer to Figure 8C).
- 84 hours after THP-1 cells were irradiated, the cell viability for the control is 71%, for GNP only is 65%, and for Glu-GNPs is 52% (refer to Figure 5C).

We stopped the experiments at 84 hours because we have clearly observed a tumor suppression trend (cells with Glu-GNPs plus irradiation achieved the best tumor suppression effect).

The following conclusions can be reached. i) Stronger X-ray irradiation leads to more cell death. Nine gray is better than 6 Gy in killing cancer cells. ii) Cell death increases as time elapses.

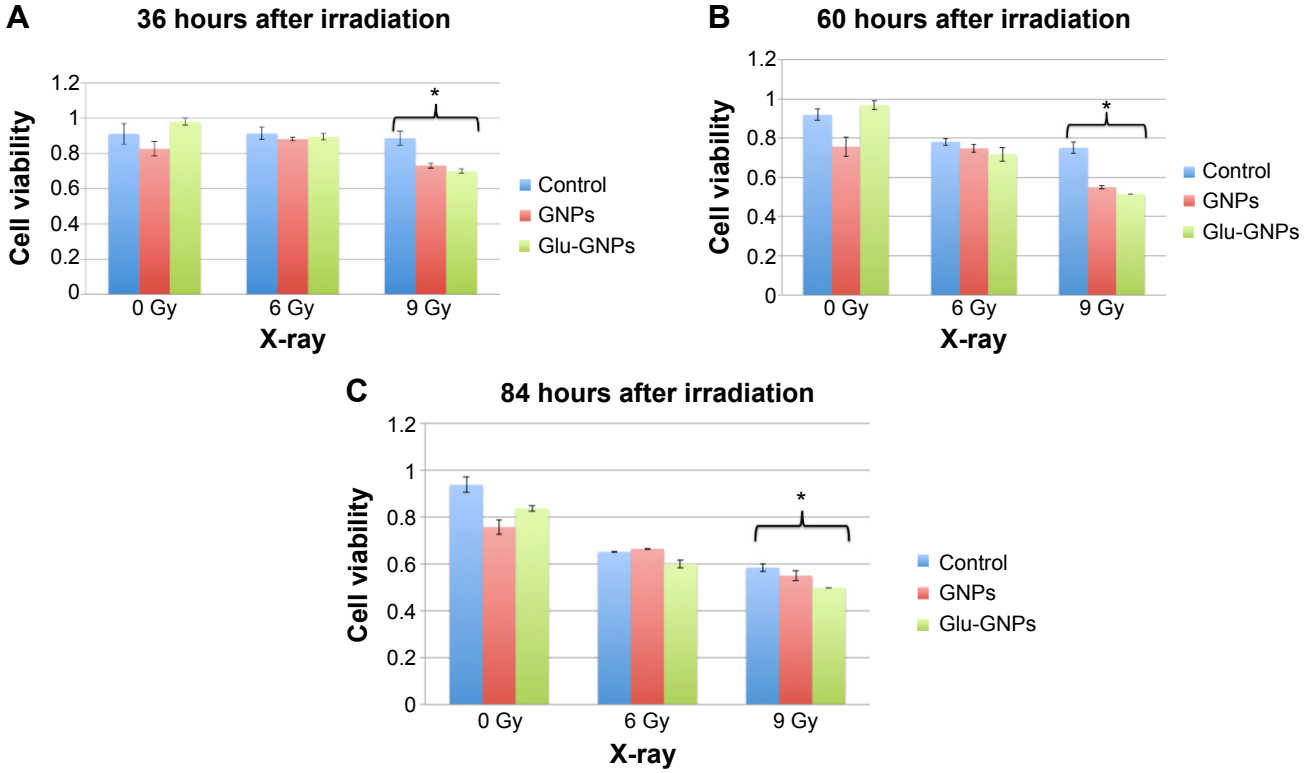

Figure 8 MCF-7 cell viability measured by cell proliferation colorimetric assay at 36 hours (**A**), 60 hours (**B**), and 84 hours (**C**) after irradiation.
Notes: *Indicates that a significant difference ($P<0.05$) was shown when comparing gold concentration of cells treated with Glu-GNPs or GNPs. Note that, on the y-axis, "1" stands for cell viability is 100%.
Abbreviations: GNPs, gold nanoparticles; Glu-GNPs, pegylated glucose coated GNPs.

iii) GNPs enhance the cancer killing. One of the most important hypotheses of this study is that GNPs can achieve better cancer killing than X-rays alone. The experimental results shown in Figure 8 validate this hypothesis. iv) Glu-GNPs can achieve better cancer killing than GNPs alone and irradiation treatment alone. The experimental results also show that cancer cells need more glucose, which leads to more Glu-GNPs entering cancer cells, resulting in more cancer cell death. Based on this study, 9 Gy irradiation should be used because 15% more cancer cells can be killed by using Glu-GNPs compared to irradiation alone (refer to the results in Figure 8B and 8C).

Glu-GNPs' enhancement of THP-1 cell killing

Figure 5A–5C shows the cell viability for THP-1 cells 36 hours, 60 hours, and 84 hours after irradiation, respectively. By comparing Figures 5 and 8, we can observe that Glu-GNPs are more effective in killing THP-1 cells than MCF-7 cells. More specifically, i) by comparing Figures 8C and 5C, the treatment effectiveness of Glu-GNP over GNP seams less evident after 84 hours for MCF-7 cells, but the treatment effectiveness of Glu-GNP over GNP appears more evident. ii) Irradiation has more immediate effectiveness on MCF-7 than THP-1 cells due to different cell characteristics. MCF-7 is an attached-growth cell, which is more sensitive to irradiation. THP-1 cell is a suspension-growth stem-like cell, which is not as sensitive to irradiation as MCF-7 cells by comparing the control in Figure 8C and the control in Figure 5C (59% vs 71%). Therefore, it is important to use nanoparticles to enhance the cell killing in order to achieve the same cancer cell killing effects (50% vs 52%). iii) Glu-GNPs can target cancer cells to get the best therapeutic effects, with at least 20% more cancer killing than treatments using GNPs alone or irradiation alone. This result can be attributed to high Glu-GNP concentration in THP-1 cells due to its suspension nature, resulting in high Glu-GNP toxicity after irradiation. SEM images of THP-1 cells with and without treatment is shown in Figure 5D. The cancer cells were damaged after treatment, which eventually led to cell death.

Clinical relevance

GNPs have high atomic number (Z=79), thus can enhance irradiation treatment because it has very high mass energy absorption compared to soft tissue. Diagnostic X-ray is often conducted at an energy level of 200 keV. However, for therapy, X-ray will have to be at much higher energies typically ranging from 1 to 15 MeV, where photon absorption in both GNPs and soft tissue is dominated by the Compton effect. In this study, both 6 Gy and 9 Gy show better cancer cell killing than the control.

According to our previous studies,[10] Glu-GNPs can enhance the irradiation effect because the accumulation of cells in G2/M phase increases from 18.4% to 29.8% 24 hours after Glu-GNP plus X-ray treatment. The possible cellular and molecular mechanisms are:

- G2/M arrest was caused by the decreased expression of p53 and cyclin A, and the increased expression of cyclin B1 and cyclin E.
- The activation of the CDK kinases induces both G0/G1 cell cycle acceleration and cell accumulation in G2/M phase.

This finding can have significant clinical implications.

Conclusion

The usefulness of GNPs and other metallic nanoparticles for cancer diagnosis and therapy has been widely reported. To the best of our knowledge, no study has been performed to test how GNPs or functional GNPs affect cancer stem cells or cancer metastasis. In this study, suspension cells (THP-1 cells in particular) were used to model cancer stem cells and metastatic cells. The cellular uptake of Glu-GNPs was evaluated and compared to that of attached cells (MCF-7 cells in particular). The results show that Glu-GNPs have a larger impact on THP-1 cells than MCF-7 cells. The average gold concentration in each THP-1 cell can be as high as about 35% more than MCF-7 cells (or $2.85*10^{-6}$ PPM vs $2.10*10^{-6}$ PPM in Figure 2). In addition, the results show that 1- to 2-hour starvation is optimal and that differential targeting effects are lost if cells are starved more than 3 hours. The X-ray results show that 9 Gy is the optimal irradiation dosage. Glu-GNPs plus X-rays can achieve better cancer killing effects (at least 20% more) compared to GNPs plus X-rays or X-rays alone. This finding can lead to better cancer treatments of cancer stem cells and cancer metastasis. In the future, these findings will be validated by animal studies and the cell cycle change of THP-1 cells.

Acknowledgments

The authors would like to say thanks for the support from Canadian Breast Cancer Research Alliance/IDEA Grant. We also would like to thank Dr Yollanda Hao and Xiaoyan Yang for their suggestions in experiment design and gold nanoparticle synthesis. Thanks also goes to Guangcheng Chen for helping with the use of the ICP-AES. Special thanks also goes to Ray Yang and Scott MacKay for proofreading the manuscript.

Disclosure

The authors have no conflicts of interest or financial ties to disclose.

References

1. Dunn GP, Bruce AT, Ikeda H, Old LJ, Schreiber RD. Cancer immunoediting: from immunosurveillance to tumor escape. *Nat Immunol*. 2002;3(11):991–998.
2. Fidler IJ. The Pathogenesis of Cancer Metastasis: the 'Seed and Soil' Hypothesis Revisited. *Nat Rev Cancer*. 2003;3(6):453–458.
3. Psaila B, Lyden D. The Metastatic Niche: Adapting the Foreign Soil. *Nat Rev Cancer*. 2009;9(4):285–293.
4. Crowe DL, Shuler CF. Regulation of Tumor Cell Invasion by Extracellular Matrix. *Histol Histopathol*. 1999;14(2):665–671.
5. Chambers AF, Groom AC, MacDonald IC. Dissemination and growth of cancer cells in metastatic sites. *Nat Rev Cancer*. 2002;2(8):563–572.
6. Reya T, Morrison SJ, Clarke MF, Weissman IL. Stem cells, cancer, and cancer stem cells. *Nature*. 2001;414(6859):105–111.
7. Dykman L, Khlebtsov N. Gold nanoparticles in biomedical applications: recent advances and perspectives. *Chem Soc Rev*. 2012;41(6):2256–2282.
8. Wang M, Thanou M. Targeting nanoparticles to cancer. *Pharmacol Res*. 2010;62(2):90–99.
9. Kong T, Zeng J, Wang X, et al. Enhancement of radiation cytotoxicity in breast-cancer cells by localized attachment of gold nanoparticles. *Small*. 2008;4(9):1537–1543.
10. Roa W, Zhang X, Guo L, et al. Gold nanoparticle sensitize radiotherapy of prostate cancer cells by regulation of the cell cycle. *Nanotechnology*. 2009;20(37):375101.
11. Geng F, Song K, Xing JZ, et al. Thio-glucose bound gold nanoparticles enhance radio-cytotoxic targeting of ovarian cancer. *Nanotechnology*. 2011;22(28):285101.
12. Kim B, Rutka JT, Chan W. Nanomedicine. *N Engl J Med*. 2010;363(25):2434–2443.
13. Murphy JC, Gole MA, Stone WJ, et al. Gold Nanoparticles In Biology: Beyond Toxicity To Cellular Imaging. *Acc Chem Res*. 2008;41(12):1721–1730.
14. Daniel MC, Astruc D. Gold Nanoparticles: Assembly, Supramolecular Chemistry, Quantum-Size-Related Properties, and Applications Toward Biology, Catalysis, And Nanotechnology. *Chem Rev*. 2004;104(1):293–346.
15. Kawasaki ES, Player A. Nanotechnology, nanomedicine, and the development of new, effective therapies for cancer. *Nanomedicine*. 2005;1(2):101–109.
16. Kim SC, Ahn Y, Wilder-Smith P, Oh S, Chen Z, Kwon YJ. Efficient And Facile Delivery Of Gold Nanoparticles In Vivo Using Dissolvable Microneedles For Contrast-Enhanced Optical Coherence Tomography. *Biomed Opt Express*. 2010;1(1):106–113.
17. El-Sayed HI, Huang XH, El-Sayed MA. Surface Plasmon Resonance Scattering and Absorption of Anti-Egfr Antibody Conjugated Gold Nanoparticles in Cancer Diagnostics: Applications In Oral Cancer. *Nano Lett*. 2005;5(5):829–834.
18. Adler CD, Huang S, Huber R, Fujimoto GJ. Photothermal Detection Of Gold Nanoparticles Using Phase-Sensitive Optical Coherence Tomography. *Opt Express*. 2008;16(7):4376–4393.
19. Beermann J, Novikov MS, Leosson K, Bozhevolnyi IS. Surface Enhanced Raman Imaging: Periodic Arrays And Individual Metal Nanoparticles. *Opt Express*. 2009;17(15):12698–12705.
20. Dragoni S, Franco G, Regoli M, et al. Gold Nanoparticles Uptake and Cytotoxicity Assessed on Rat Liver Precision-Cut Slices. *Toxicol Sci*. 2012;128(1):186–197.
21. Cheng Y, Samia CA, Meyers DJ, Panagopoulos I, Fei B, Burda C. Highly Efficient Drug Delivery With Gold Nanoparticle Vectors for In Vivo Photodynamic Therapy Of Cancer. *J Am Chem Soc*. 2008;130(32):10643–10647.
22. Paciotti FG, Myer L, Weinreich D, et al. Colloidal Gold: A Novel Nanoparticle Vector for Tumor Directed Drug Delivery. *Drug Deliv*. 2004;11(3):169–183.
23. Cheng Y, Meyers DJ, Agnes SR, et al. Addressing Brain Tumors with Targeted Gold Nanoparticles: A New Gold Standard for Hydrophobic Drug Delivery. *Small*. 2011;7(16):2301–2306.
24. Paciotti FG, Kingston D, Tamarkin L. Colloidal Gold Nanoparticles: A Novel Nanoparticle Platform for Developing Multifunctional Tumor-Targeted Drug Delivery Vectors. *Drug Development Research*. 2006;67(1):47–54.
25. Choi CH, Alabi AC, Webster P, David ME. Mechanism Of Active Targeting In Solid Tumors With Transferrin-containing Gold Nanoparticles. *Proc Natl Acad U S A*. 2010;107(3):1235–1240.
26. Chen JY, Wang DL, Xi JF, et al. Immuno Gold Nanocages with Tailored Optical Properties for Targeted Photothermal Destruction of Cancer Cells. *Nano Lett.* 2007;7(5):1318–1322.
27. Dorsey JF, Sun L, Joh DY, et al. Gold nanoparticles in radiation research: potential applications for imaging and radiosensitization. *Transl Cancer Res*. 2013;2(4):280–291.
28. Jain S, Coulter JA, Hounsell AR, et al. Cell-specific radiosensitization by gold nanoparticles at megavoltage radiation energies. *Int J Radiat Oncol Biol Phys*. 2011;79:531–539.
29. Berbeco RI, Ngwa W, Makrigiorgos GM. Localized dose enhancement to tumor blood vessel endothelial cells via megavoltage X-rays and targeted gold nanoparticles: new potential for external beam radiotherapy. *Int J Radiat Oncol Biol Phys.* 2011;81(1):270–276.
30. Zhang X, Xing JZ, Chen J, et al. Enhanced radiation sensitivity in prostate cancer by gold-nanoparticles. *Clin Invest Med*. 2008;31(3):E160–E167.
31. Butterworth KT, McMahon SJ, Taggart LE, Prise KM. Radiosensitization by gold nanoparticles: effective at megavoltage energies and potential role of oxidative stress. *Transl Cancer Res*. 2013;2(4):269–279.
32. Raya SB, Wahl LR. Overexpression of glut-1 glucose transporter in human breast cancer an immunohistochemical study. *Cancer*. 1993;72(10):2979–2985.
33. Larson TA, Joshi PP, Sokolov K. Preventing protein adsorption and macrophage uptake of gold nanoparticles via a hydrophobic shield. *ACS Nano*. 2012;6(10):9182–9190.
34. Jain S, Coulter JA, Butterworth KT, et al. Gold nanoparticle cellular uptake, toxicity and radiosensitisation in hypoxic conditions. *Radiother Oncol*. 2014;110(2):342–347.
35. Praetorius NP, Mandal TK. Engineered Nanoparticles in Cancer Therapy. *Recent Pat Drug Deliv Formul*. 2007;1(1):37–51.
36. Conde J, Doria G, Baptista P. Noble Metal Nanoparticles Applications in Cancer. *J Drug Deliv*. 2012;2012:751075.
37. Kaur H, Pujari G, Semwal MK, Sarma A, Avasthi DK. In Vitro Studies On Radiosensitization Effect Of Glucose Capped Gold Nanoparticles In Photon and Ion Irradiation of Hela Cells. *Nuclear Instruments and Methods in Physics Research Section B Beam Interactions with Materials and Atoms*. 2013;301:7–11.
38. Su S, Zuo X, Pan D, et al. Design and Applications of Gold Nanoparticle Conjugates by Exploitin Biomolecule – Gold Nanoparticle Interactions. *Nanoscale.* 2013;5(7):2589–2599.
39. Macheda ML, Rogers S, Best JD. Molecular and cellular regulation of glucose transporter (GLUT) proteins in cancer. *J Cell Physiol*. 2005;202(3):654–662.
40. Calvo BM, Figueroa A, Pulido EG, Campelo RG, Aparicio AL. Potential Role of Sugar Transporters in Cancer and Their Relationship with Anticancer Therapy. *Int J Endocrinol*. 2010;2010.pii:205357.
41. Geng F, Kong B, Xing JZ, Chen J. Enhancing Multimodality Functional and Molecular Imaging Using Glucose Coated Gold-nanoparticles. *Clin Radiol*. 2014;69(11):1105–1111.
42. Roa W, Xiong Y, Chen J, et al. Pharmacokinetic and toxicological evaluation of multi-functional thiol-6-fluoro-6-deoxy-D-glucose gold nanoparticles in vivo. *Nanotechnology*. 2012;23(37):375101.
43. Benício MT, Scheucher PS, Garcia AB, Falcao RP, Rego EM. Characterization Of Leukemic Stem Cells In AML Cell Lines Using ALDH Staining. *Blood*. 2013;122(21):5409.
44. Bases R. Clonogenicity of human leukemic cells protected from cell-lethal agents by heat shock protein 70. *Cell Stress Chaperones*. 2005;10(1):37–45.

45. Gee K, Lim W, Ma W, et al. Differential regulation of CD44 expression by lipopolysaccharide (LPS) and TNF-alpha in human monocytic cells: distinct involvement of c-Jun N-terminal kinase in LPS-induced CD44 expression. *J Immunol*. 2002;169(10):5660–5672.
46. Geng F, Xing JZ, Chen J, et al. Pegylated Glucose Bound Gold Nanoparticles for Improved In-vivo Bio-distribution and Enhanced Radiotherapy on Cervical Cancer. *J Biomed Nanotechnol*. 2014;10(7):1205–1216.
47. Arya SK, Lee KC, Dah'alan B, Rahman AR. Breast tumor cell detection at single cell resolution using an electrochemical impedance technique. *Lab Chip*. 2012;12(13):2362–2368.
48. Muñoz-Pinedo C, Mjiyad N, Ricci JE. Cancer metabolism: current perspectives and future directions. *Cell Death Dis*. 2012;3:e248.
49. Huang SD, Yuan Y, Liu XH, et al. Tumor Cells Positive and Negative for the Common Cancer Stem Cell Markers Are Capable of Initiating Tumor Growth and Generating Both Progenies. *PLoS One*. 2013;8(1):e54579.
50. Griffiths A, Gelbart W, Wessler S. *An Introduction to Genetic Analysis*. 8th ed. W.H. Freeman & Company; 2004.
51. Kindt T, Osborne BA, Goldsby RA. *Kuby Immunology*. 6th ed. W.H. Freeman & Company; 2006.